Influence of dynamic copper speciation on bioavailability in streams

Basic Information

Title:	Influence of dynamic copper speciation on bioavailability in streams
Project Number:	2012CT259B
Start Date:	3/1/2012
End Date:	2/28/2014
Funding Source:	104B
Congressional District:	CT-002
Research Category:	Water Quality
Focus Category:	None, None, None
Descriptors:	None
Principal Investigators:	Timothy Vadas

Publication

1. Luan, H. and T.M. Vadas. 2012. Cu lability and bioavailability in an urban stream during baseflow versus stormflow. American Geophysical Union Annual Conference. San Francisco, CA. Dec 2012.

Proposal Title: Influence of dynamic copper speciation on bioavailability in streams

Introduction

Copper is both an essential micronutrient for biology and a potential toxicity issue at high concentrations. Besides the natural sources of Cu in ecosystems that provide nutrition, there are many additional anthropogenic sources that are reaching receiving water bodies, including dissolved Cu from roofing materials, household water distribution pipes, applications of copper sulfate algicides, abrasion of brake pads and other commercial uses (Marsalek et al., 1999). Within a given reach of a stream, there are potentially four contributing sources of Cu, including wastewater treatment plant effluent (industrial or municipal), stormwater inputs, legacy pollution in the sediments, and Cu in baseflow that may be contributed by natural sources or e.g., by algicide application upstream.

Although for impaired water bodies regulations focus on total pollutant input to receiving water bodies regardless of its chemical form, Cu speciation influences bioavailability, and thus stream impairment due to toxicity and changes in ecosystem function. Cu speciation is controlled primarily by organic matter and introduces a level of complexity in understanding bioavailability. While in select cases, uptake of DOC-metal complexes may have occurred (Campbell et al., 2002; Vadas and Ahner, 2009), in most cases, uptake is thought to be controlled by diffusion, lability and transfer of the free metal to a transporter on the cell surface. Based on that, the major conditions that control the uptake of Cu in urban streams are either the diffusion of labile complexes or the kinetics of metal-ligand complex exchange. The equilibrium condition of this model is considered in the biotic ligand model. However, when considering the biological structure of a stream ecosystem, dietary uptake needs to be considered. While biological uptake may still be controlled by the strength and kinetics of the organic ligand, both the dynamic conditions in streams and the food web structure can influence biouptake and trophic transfer, e.g. metal attachment and uptake in periphyton and trophic transfer to grazers.

The research conducted focuses on Cu contamination, which is of widespread concern across the state of Connecticut, including for example the Eagleville Brook watershed surrounding part of UConn campus, the Hockanum River or the Tankerhoosen River watershed. Many TMDLs developed or in development in the state currently utilize acute and chronic water quality standards to set total copper loads and/or whole effluent toxicity studies. However, these have not always been sufficient to reduce impairment, most likely due to differences in chronic toxicity. Future analyses will be better served to assess loads based on aqueous phase copper speciation criteria with a causal link to biological impacts. This can only be accomplished by understanding the dynamic conditions in urban streams, and the relationship of Cu speciation with biological uptake.

With respect to metal source, the current assessment of total and dissolved Cu ignores relevant speciation information that may inform mechanisms of impairment. Speciation measurements are not simple or routine and thus would not be appropriate for regulatory use. In an effort to get around that issue, chemical surrogates such as diffusive gradients in thin film (DGT) devices have been developed that measure "bioavailable" metals (Zhang and Davison 2000). These have been validated for soil systems and plant root bioavailability, but their use in waters and sediments as stream organism uptake indicators has not been validated (Warnken et al., 2008). Ultimately, what DGT devices will measure in streamwater are labile species, i.e. readily exchangeable Cu that could potentially interact with a biotic ligand as an indicator of biologically available metals.

In addition to passive chemical sensors, periphyton have been used to assess metal uptake in streams (Meylan et al 2003). Periphyton is the most important primary producer in running waters and responsible for the uptake and retention of organic carbon and inorganic nutrients. Periphyton, being one trophic level

below macroinvertebrates, should more accurately capture the dynamic conditions in streams and help pinpoint the source and timing of contaminants that lead to impairment of the water body.

In summary, the goal of the research was to assess two tools to measure bioavailable metals in streams, DGT and periphyton cultures. These were assessed in combination with water chemistry measurements as well as characterization of metal size distribution in different source waters to the stream. These were assessed both as a function of distance downstream of the inputs in the case of effluent as well as over the course of several storm events, two pieces of information that are not currently captured using grab samples or macroinvertebrate surveys. The data suggests a strong difference between bioavailability of effluent sources versus stormwater sources and further studies should be conducted to assess a wider range of source waters and seasonal variability. These simple assessment tools could be used to provide justification for management decisions based on Cu speciation, not just total Cu, and mitigation options based on source and location of inputs.

Research Objectives:
Results from this work have implications for improving risk assessment at impacted sites, enhancing dynamic bioaccumulation models, and providing evidence for reducing their impacts through treatment or restoration activities that manage carbon or metal sources. This research addressed three specific questions:

1) What is the impact of the dynamic urban stream environment on metal size speciation?
2) Can a chemical surrogate readily predict biouptake in a benthic organism?
3) Do anthropogenic metal sources drive excess biouptake in stream organisms?

Methods

Site description
The Hockanum River (Connecticut, USA) originates at the outlet of Shenipsit Lake and flows 36.4 km through Vernon, Ellington, Manchester, and East Hartford before it spills into Connecticut River. This research mainly investigated the reach flowing through Vernon, which is primarily a suburban area. The Hockanum River was contaminated by Cu inputs from base flow, stormwater, and treated wastewater. The Hockanum River which flows through the towns of Vernon and Manchester had an average flow rate of 3.94 m^3/s over the last few years. A water pollution control facilities (WPCF) in Vernon discharges treated effluent into the river, with an average effluent discharges of 0.21 m^3/s. In addition, separate storm sewers exist and discharge into the river in several locations along its course. Six sampling locations were selected to deploy the diffusive gradient in thin film (DGT) and periphyton samples from upstream to downstream along the Hockanum river, including one in Rockville, the wastewater treatment plant (WWTP) upstream and downstream, Dart Hill Road, Hockanum Blvd, and Pleasant View Dr. The storm runoff was collected from the discharge pipe at Pleasantview Dr (Figure
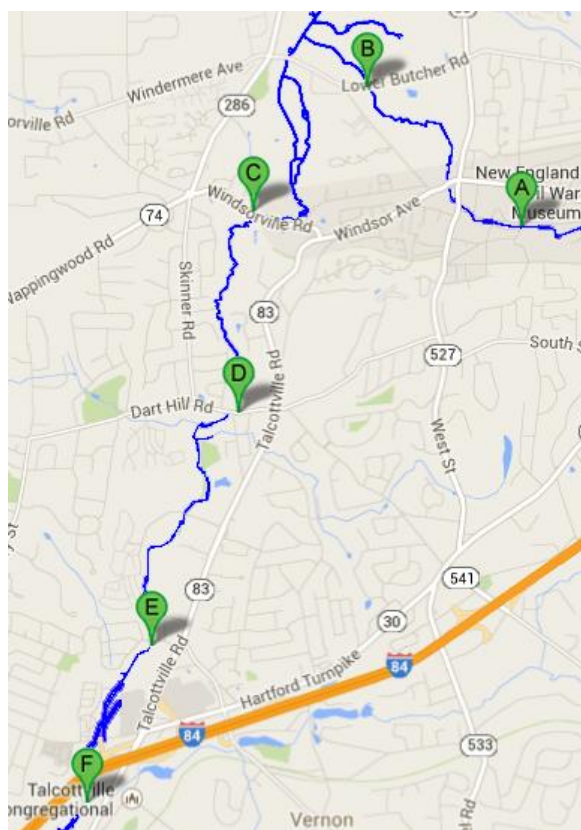

Figure 1: Hockanum River sampling locations

1). Additonal grab samples for size distribution comparison were taken from the Quinnebaug River, Willimantic River, and associated wastewater treatment plants.

Passive sampler preparation
Microscope slides pre-loaded to acrylic racks were used to colonize periphyton. To minimize collection of suspended particles, the racks were deployed vertically about 10 cm below the water surface. 4 racks holding 16 microscope paired slides each were placed next to each other parallel to the water current. A 3-week colonization period in a clean water source prior to use was necessary to obtain sufficient periphyton. DGT-devices were made following the procedure described by Zhang (2000). To get a consistent performance, the thickness of diffusive gel was modified to 1.0 mm.

Sampling and sample preparation
Water samples were collected in acid washed low density polyethylene (LDPE) bottles for dissolved, colloidal and total metal concentration, dissolved organic carbon (DOC) and alkalinity. DGT devices were deployed 10 cm above the bottom of the river and retrieved after 24 h exposure. Periphyton slides were deployed in the same way but retrieved at certain time intervals along the storm event. Water, periphyton and DGT sampling was performed before, during and after several storm events as well as a function of distance downstream from the WWTP during baseflow. At the time of sampling, 4 microscope slides were thoroughly rinsed with filtered river water (0.45 μm). The natural algal biofilm was then scratched from the slide with a clean microscope slide and was suspended in filtered river water. The suspension was afterward divided into two fractions. One fraction (20 mL) was treated for 10 min with 4.0 mM EDTA to remove the metals adsorbed to the cell wall and most of the inorganic complexes embedded in the biofilm. This process allowed for the measurement of the intracellular metal content of periphyton. The other fraction was used to measure the total metal accumulated in periphyton. The difference between total and intracellular metal content is considered to be adsorbed metal on periphyton. Three aliquots of each fraction were filtered with acid-washed and preweighed filters (cellulose nitrate 0.45 μm) to obtain the dry weight (dw) of each sample after drying to a constant weight at 50 °C. The filters were digested following standard methods (EPA Method 3050B). Briefly, the filters were soaked in 4 mL of concentrated nitric acid (ACS) in a 15 mL digestion tube. Digestion samples were heated at 95 °C±5°C until no brown fumes were given off. Subsequently, hydrogen peroxide (30%) was added stepwise until the effervescence was minimal or until the general sample appearance was unchanged. The digested sample was diluted for ICP analysis. Water samples for dissolved metals and DOC were also filtered through 0.45 μm nitrocellulose filters then pH adjusted to 2 with nitric or hydrochloric acid, respectively. For DGT devices, after retrieval from the field, the resin gel was peeled off and transferred to an acid-cleaned 2 mL microcentrifuge tube containing 1mL of 1M HNO_3 and soaked overnight. The elution solution was diluted 5 times with 1% HNO_3 matrix prior to analysis on ICP-MS.

Size distribution by AFFFF coupled to ICP-MS
Concentration and size distribution of colloidal metal complexes was characterized by asymmetric flow field flow fractionation (AF4, Postnova Analytics, Landsberg, Germany) coupled on-line to UV detection at 254 nm for aromatic DOC determination and ICP-MS for trace metal determination. The AF4 2000 Control software (Postnova Analytics) was used for data collection and analysis of UV signals and size calculations, while Agilent Chemstation (MassHunter) software was used for time resolved analysis of metals. Prior to injection into the ICP-MS introduction system, a 6% nitric acid solution containing 500 ppb Sc was mixed in as an internal standard and to acidify the neutral samples. The AF4 system was metal free and equipped with a 275 mm long trapezoidal channel cartridge and different size spacers depending on the method. The mobile phase was 10mM $NaNO_3$ with pH matched to the source water. Samples were analyzed in two different modes, to capture more resolution in the large or small size colloidal fractions. Capture of the large size fraction was achieved using a 10 kDa cut-off polyethersulfone (PES) membrane and a 350 μm spacer. Samples were injected to the channel using a 1 mL sample loop at an injection flow of 0.2 mL min^{-1} for 6 min. After a 1 min transition time, samples

were separated using a channel flow of 1 mL min^{-1} and a constant cross flow of 1 mL min^{-1} over 40 minutes. To capture the small size fraction, a 300 Da cut-off PES membrane was used with a 500 μm spacer. The 300 Da membrane was selected over the typically used 1 kDa PES or 1 kDa regenerated cellulose membranes because it had the most metal recovery, i.e. limited metal retention on the membrane, from the various water sources when analyzed without crossflow.

Sample analysis
Inductively coupled plasma-mass spectrometry (ICP-MS, Agilent 7700x, Agilent, USA) was applied for determination of the metals in this work. A total organic carbon analyzer (Apollo 9000, Tekmar-Dohrmann, USA) was used to measure dissolved organic carbon (TOC).

Results:

Metal distribution between particulate, colloidal and truly dissolved fractions
        The bulk metal distributions in in stream, effluent and stormwater samples showed large variations. Upstream and stormwater samples usually had more total Fe and higher colloidal Fe fractions than the effluent, with the exception of H_up (Fig 2). More than 30% of Fe was present in the particulate form especially for the stormwater (above 60%) which strongly correlates with particulate Pb concentrations in solution. On the other hand, the effluent and stormwater samples had much higher Cu and Zn concentrations than the upstream samples. Cu and Zn were mostly found in the truly dissolved fractions (usually >50%), 20-50% in the colloidal phase, and a typically smaller fraction in the particulate phase
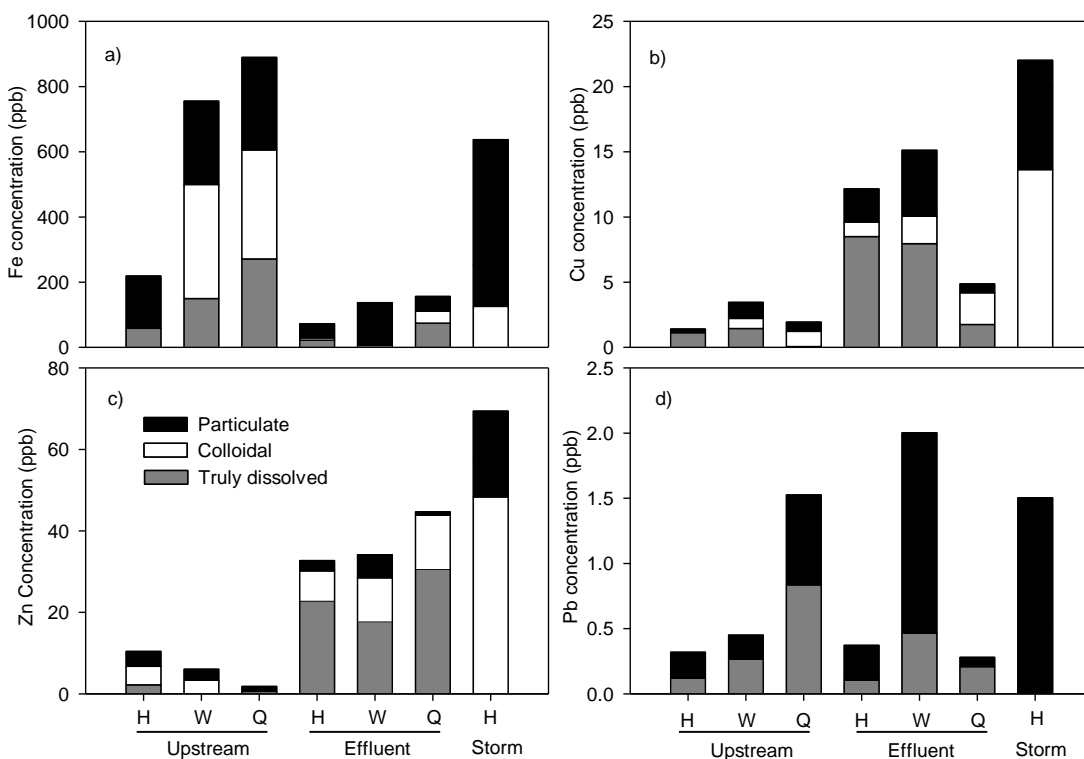

Figure 2: Size distribution between particulate, colloidal and truly dissolved in stream, effluent and storm runoff samples

which is similar to previous observations of effluent sources (Worms et al., 2010). The colloidal size fraction, which can contain up to 50% of the dissolved metals, covers a large size distribution, and samples were further analyzed to assess the metal association between organic matter and iron colloids.

Colloidal size distribution of metals

The colloidal fractions of Fe in Q_up and W_up showed both small (0.5-3 nm; 10-20% of the mass) and much more dominant large (3-80 nm; 70-80% of the mass) size distributions (data not shown), whereas Fe in effluent samples was only observed in the small size range. The large size fraction of Fe never co-eluted with UV measurable organic matter or other metals measured in this study, and was likely primarily composed of iron oxides (Perret et al., 2000; Stolpe et al., 2013). The only observable difference in the large size range Fe was a broader peak in the Q_up compared to the W_up which could have been due to differences in stream velocity or water chemistry. Further analysis focused on a higher resolution analysis of the smaller size range colloids with both metals and organic matter present.

For all samples measured via AF4-ICP-MS, the majority of colloid associated metals, besides Fe, were found in the less than 3 nm size range. However, the distribution and association with OM or Fe was different depending on the metal. The size distributions of UV-absorbance, as a surrogate for OM, showed two peaks in both effluent and upstream samples, one centered around 0.5 nm and one typically larger peak centered around 2 nm (Fig. 3, upstream data not shown). The Fe signal exhibited a similar pattern for upstream samples, but the magnitude of the 0.5 nm peak was larger for Fe. The smaller size range of OM corresponded to molecular weights of less than 1 kDa, while the larger size range fell between 1 kDa and 50 kDa. The smaller size fraction is likely more fulvic-rich, while the larger size is likely a mixture of fulvic and humic acids? (Beckett et al., 1987). Only a few subtle differences existed between effluent and upstream samples. In effluent samples, while the size distribution of UV absorbance still showed two peaks, the magnitude of the signals decreased and the maximum of the second peak shifted to a lower kDa size range in W_eff and H_eff samples. Even though DOC concentrations were of the same order of magnitude for upstream and effluent samples, organic matter from effluent is typically skewed to the smaller size range. The fulvic acid signal observed in the EEMs spectra for effluent samples was not as strong as upstream samples, thus this smaller size contribution likely comes from the much larger protein enriched signals observed in effluent. The size distribution of the Q_eff organic matter remained similar to the upstream waters. The first peak of Fe was mostly absent or non-detectable in the effluent samples as expected from the size distribution results (Fig 2), and the maximum of the second peak was more closely associated with organic carbon. While the relative metal mass in the two size ranges differed between samples, they each overlapped, suggesting the presence of either an organic matter bound Fe ion, or an iron oxide and organic matter aggregate.

Most of the single peaks of Pb and Zn in effluent and upstream samples fell between the peaks of Fe and OM, suggesting some binding to both size ranges of colloids, while the single peak of Cu lined up directly with the UV signal, but also overlaps a portion of the Fe
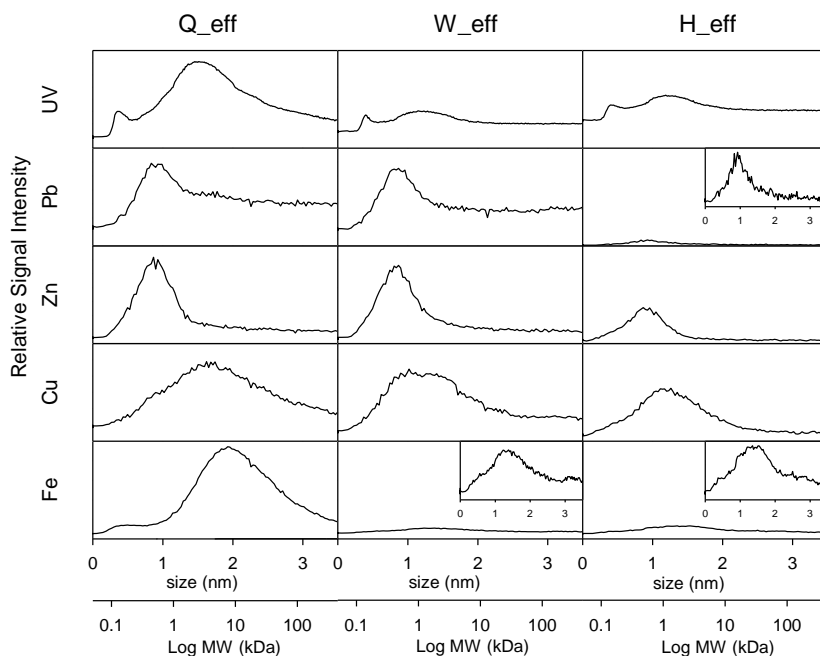

Figure 3: Colloidal size fractionation of metals and organic matter in effluent samples

5

signal (Fig. 3, upstream data not shown). The Zn and Pb signals in particular had long shoulders in the larger size range, similar to the UV signal. Only in the H_up samples were the Pb and Zn peaks aligned with the UV signal, but these were much lower concentrations and in that case there was very little colloidal Fe present. The strong association with organic matter was expected for Cu (Tipping, 1998) , while Pb typically associates with iron oxides, and Zn association falling somewhere in between. However, since all signals overlap, there are likely a variety of associations present, e.g. mixed aggregates of iron oxides, organic matter, and metals bound to organic ligands or iron oxide surfaces.

During the storm event, all colloidal metal and UV peaks showed variation in magnitude, and Fe and Pb in particular showed shifts in size distributions over time. The colloidal size distributions of Fe in stormwater samples collected during the first hour were predominated by a single peak centered at about 2 nm, extending over a slightly larger range of sizes compared to the upstream or effluent samples. More than an hour after the storm started, Fe in even larger size ranges were observed, with a peak around 5 nm with a long tail extending into larger size distributions increasing over time. Meanwhile, the size distribution of UV-absorbance only exhibited one single peak at all times centered around 1-10 kDa, similar to the upstream and effluent samples, but the magnitude increased by a factor of 3 from the earlier to later times of stormwater runoff. This is consistent with the generally higher SUVA values observed later in the storm (Table 1). The colloidal size distributions of Cu and Zn are similar throughout the storm event, only varying in magnitude with the highest concentrations observed later in the storm and the lowest observed in the first 45 min? During the storm, both Cu and Zn are more closely associated with organic matter, though Zn peaks at a slightly lower size. The size distribution of Pb is a lot less uniform and varies significantly over time. In the first 30 min, the size distribution was very broad, spanning a size range of about 1-5 nm, and exhibited a double peak (data not shown). The two peaks correspond to the peaks in UV and Fe, suggested a role of both organic matter and iron oxides in binding Pb during a storm. Over time, the peaks change and shift in relative magnitude and are shifted to the lower size range later in the storm. The colloidal metal concentrations decreased for the first 45 minutes then increased, following the same trend as the dissolved metal concentrations in storm runoff. This shift in metal concentrations was likely due to differences in sources and transport times in the stormdrain system. The appearance of larger size colloidal Fe and the increased Fe and DOC concentrations could have been released from the upper organic-rich soil horizons because the size of the second peak was similar to the typical colloids found in the soil pore-water (Pokrovsky et al., 2005; Stolpe et al., 2013). It is also possible that iron oxide formation or aggregation processes during the travel time resulted in the about 3-fold increase in colloidal Fe concentration over the course of the storm.

Alterations in colloidal distributions upon mixing and spiking

Since these source waters all mix in the receiving stream, we assessed changes in colloidal metal distribution and size upon mixing with stream water or upon addition of metals or competing cations. The size distributions of mixed samples (H_up:H_eff of 7:3 or H_up:H_st of 1:1) were similar to the calculated distribution based on the previously measured individual sample distribution and mixing ratio. This suggests the colloids originally present in the source water are maintained upon entering stream waters. Spiking samples with Cu, Zn and Pb at 10-fold background concentrations revealed differences depending on the metal. Colloidal Cu increased proportionally, but the size distribution and association with organic matter changed little with the exception of a longer tail on the peak. The percentage of colloidal Cu remained the same in effluent, but decreased from 30 to 15% in stormwater samples, suggesting that even though the concentration of organic matter was lower in effluent mixture, it still had excess binding capacity compared to the stormwater. The percent colloidal Zn was already low in the samples and spiking did not significantly increase its concentration and it remained in the small size range. The addition of excess Ca did not alter the size distribution or colloidal phase concentrations in effluent mixtures, but did significantly change the stormwater mixtures. At a doubling of the Ca concentration, the total colloidal metal concentration slightly increased, possibly due to enhanced bridging of smaller organic matter. However, at a 10-fold increase in Ca concentration, the total colloidal metal concentration

was reduced and the size distribution shifted to the smaller size range, likely due to competition at ligand binding sites.

Periphyton and DGT response during baseflow
During baseflow, water, DGT, and periphyton samples were collected as a function of distance downstream. These samples were collected during July and August, when WWTP effluent contributed approximately 35% of the stream flow. Dissolved and total Cu concentrations were approximately 2 ppb upstream of the wastewater treatment plant and 5 ppb downstream of the wastewater treatment plant. The DGT labile portion of the streamwater Cu was about 25-30% upstream of the WWTP and increased to about 40% immediately downstream of the effluent outfall (Fig. 4). The DGT labile portion continued to increase as water flowed downstream, up to a maximum of about 50%. This occurred even though the Cu concentration did not change significantly as water traveled downstream. This suggests some transformation of the effluent organic matter that binds Cu, resulting in more Cu lability further downstream. The periphyton body burden for the most part followed the same trend as DGT labile Cu, with the exception of the furthest location downstream. Upstream periphyton had body burdens of about 15-30 ug/g intracellular Cu, while immediately downstream they increased to about 40 ug/g and total periphyton Cu increased further downstream. However, the furthese location had body burdens similar to the upstream site.
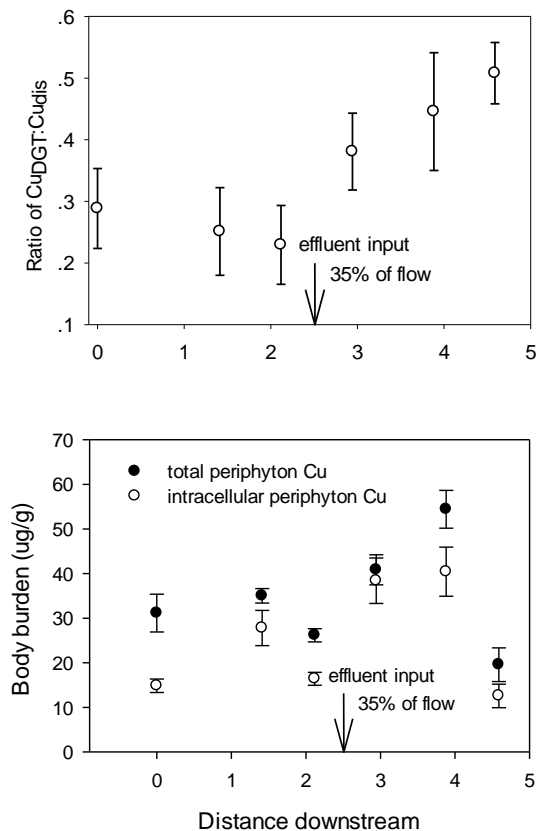

Figure 4: Labile Cu ratio and periphyton body burden as a function of distance downstream

Periphyton and DGT response during stormflow
A total of five different storm events were observed during the fall of 2012 and 2013. Results from one example event are shown in Figures 5 and 6. Prior to the storm, the periphyton body burdens upstream of the WWTP were similar to baseflow conditions from the previous summer, arounb 30 ug g^{-1}. Following a storm even, the total and dissolved Cu and DOC concentrations spiked for a period of about 2 days and periphyton body burdens increased to more than 50 ug g^{-1}. This level remained over 50 ug g^{-1}, but varied over time, decreasing four days after the storm, but increasing again following another small increase in water column Cu concentration. Generally, total periphyton Cu concentrations were elevated, but followed intracellular Cu concentrations over time. Each time the periphyton body burden increased, the DGT labile Cu concentration from the previous days was elevated, suggesting it was a reliable indicator of bioavailable Cu at the upstream site.

At the site furthest downstream of the WWTP, periphyton body burden was initially about 50 ug g^{-1}, again similar to the baseflow conditions downstream of the WWTP. Following the storm event, there was a smaller spike in DOC and Cu concentrations, and the DOC concentration remained slightly elevated around 4 to 5 mg L^{-1}, but the Cu concentration generally remained similar, about 3 to 4 ug L^{-1}.
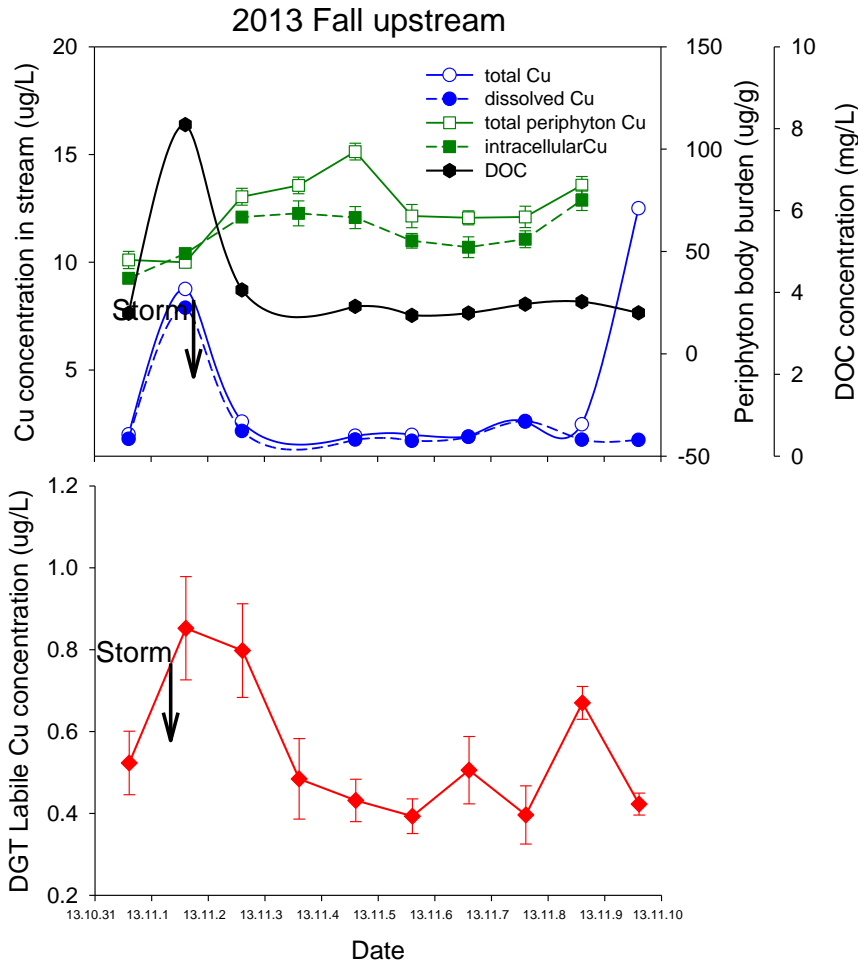

Figure 5: Dynamics of water chemistry and periphyton response to a storm even upstream of the wastewater treatment plant

This concentration was still elevated compared to the upstream site, however periphyton body burden did not start to significantly increase until about 4 days after the storm, increasing to about 120 ug g^{-1} at the highest point. However, there was significant day to day variability, with intracellular body burdens ranging from about 70 to 120 ug g^{-1}, and remaining elevated for more than a week following the storm. In this event, the DGT labile Cu concentration was highest initially, and started to decrease following the storm, possibly due to dilution with less labile Cu sources. This might suggest the largest increase in periphyton body burden should have occurred during the days during and immediately following the storm event, but that didn't happen. Perhaps the increase in periphyton body burden over time occurred due to either some transformation of the particulate Cu concentrations over time, or a kinetically limited uptake process dependent on the Cu speciation or size distribution embedded in the extracellular matrices.

Environmental Significance

The DGT devices generally followed the periphyton body burden during baseflow and upstream water exposure. However, following storm events there was not a clear relationship between the two. Based on the size distribution analysis of mixed source waters, it was common for effluent to have excess Cu binding capacity, while stormwater did not, even though it had higher concentrations. In that respect, DGT labile concentrations might be expected to increase in streams following the storm, but they generally did not. This could be due to seasonal differences in organic matter lability, i.e. grab samples for metal size distribution were taken during the peak of the growing season, while storms were monitored during the fall. In addition, following the storm event, the changes in DGT labile concentrations upstream followed the dissolved Cu concentrations, but downstream of the WWTP, there

was a more prolonged change in DGT labile concentrations, much longer after the flow returned to baseflow levels. This could be due to differences in colloid transport and settling, or dynamics of metal repartitioning onto to newly exposed or transported surfaces within the stream. The periphyton also had a much larger lag time in response to metal exposure downstream during storm events. It is difficult to identify the specific reasons in-situ, but we expect some of the response is due to differences in colloidal phase organic matter over time, interactions with periphyton surfaces, and kinetic exchange limitations on periphyton uptake. These types of interactions need to be further studied in controlled laboratory environments.
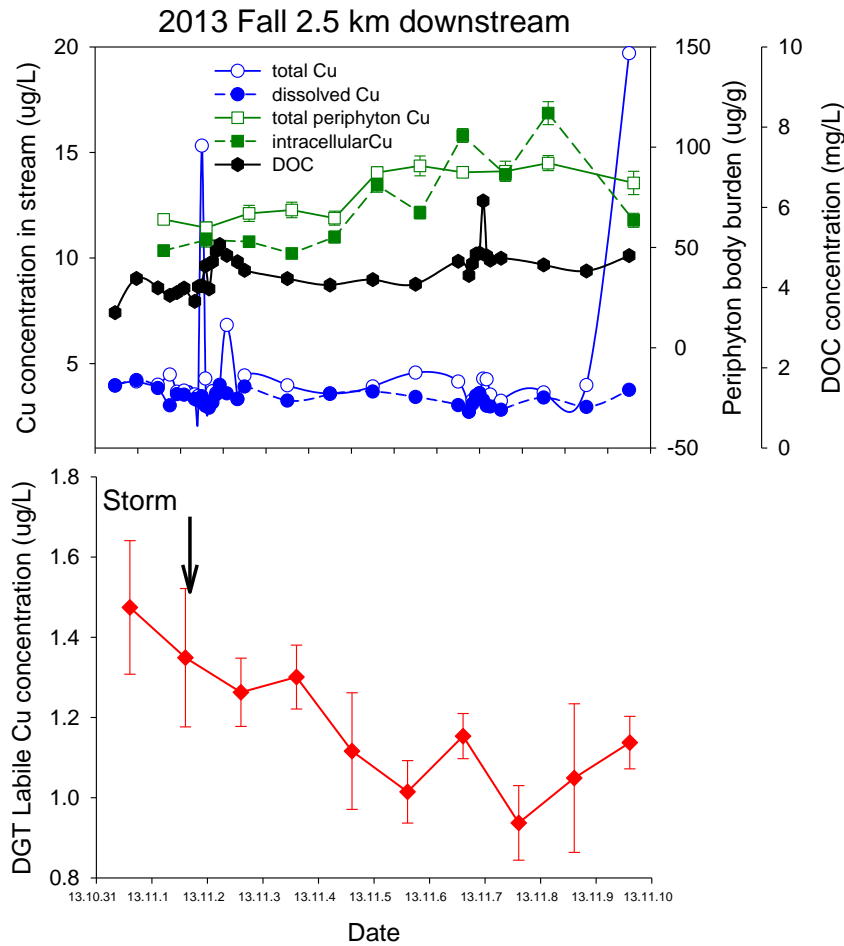

Figure 6: Dynamics of water chemistry and periphyton response to a storm even downstream of the wastewater treatment plant

References

Campbell, P.G.C., Errecalde, O., Fortin, C., Hiriart-Baer, V.P., and Vigneault, B., 2002, Metal bioavailability to phytoplankton - applicability of the biotic ligand model: Comparative Biochemistry and Physiology Part C, v. 133, p. 189-206.

Marsalek, J., Rochfort, Q., Brownlee, B., Mayer, T., and Servos, M., 1999, An explanatory study of urban runoff toxicity: Water Science and Technology, v. 39, p. 33-39.

Meylan, S., Behra, R., and Sigg, L., 2003, Accumulation of copper and zinc in periphyton in response to dynamic variations of metal speciation in freshwater: Environmental Science & Technology, v. 37, p. 5204-5212.

Pokrovsky, O.S., Dupre, B., and Schott, J., 2005, Fe-Al-organic colloids control of trace elements in peat soil solutions: Results of ultrafiltration and dialysis: Aquatic Geochemistry, v. 11, p. 241-278.

Stolpe, B., Guo, L.D., Shiller, A.M., and Aiken, G.R., 2013, Abundance, size distributions and trace-element binding of organic and iron-rich nanocolloids in Alaskan rivers, as revealed by field-flow fractionation and ICP-MS: Geochimica et Cosmochimica Acta, v. 105, p. 221-239.

Vadas, T.M., and Ahner, B.A., 2009, Cysteine and glutathione-mediated uptake of Pb and Cd into *Zea mays* and *Brassica napus* roots: Environmental Pollution, v. 157, p. 2558-2563.

Warnken, K.W., Davison, W., and Zhang, H., 2008, Interpretation of in situ speciation measurements of inorganic and organically complexed trace metals in freshwater by DGT: Environmental Science & Technology, v. 42, p. 6903-6909.

Zhang, H., and Davison, W., 2000, Direct in situ measurements of labile inorganic and organically bound metal species in synthetic solutions and natural waters using diffusive gradients in thin films: Analytical Chemistry, v. 72, p. 4447-4457.